# Activation of Methyltetrahydrofolate by Cobalamin-Independent Methionine Synthase†

Rebecca E. Taurog‡ and Rowena G. Matthews*,‡,§,||

*Department of Biological Chemistry, Life Sciences Institute, and Biophysics Research Division, The University of Michigan, Ann Arbor, Michigan 48109-1055*

*Received January 10, 2006; Revised Manuscript Received March 1, 2006*

ABSTRACT: Cobalamin-independent methionine synthase (MetE) catalyzes the final step of de novo methionine synthesis using the triglutamate derivative of methyltetrahydrofolate ($CH_3$-$H_4PteGlu_3$) as methyl donor and homocysteine (Hcy) as methyl acceptor. This reaction is challenging because at physiological pH the Hcy thiol is not a strong nucleophile and $CH_3$-$H_4PteGlu_3$ provides a very poor leaving group. Our laboratory has previously established that Hcy is ligated to a tightly bound zinc ion in the MetE active site. This interaction activates Hcy by lowering its p$K_a$, such that the thiolate is stabilized at neutral pH. The remaining chemical challenge is the activation of $CH_3$-$H_4PteGlu_3$. Protonation of N5 of $CH_3$-$H_4PteGlu_3$ would produce a better leaving group, but occurs with a p$K_a$ of 5 in solution. We have taken advantage of the sensitivity of the $CH_3$-$H_4PteGlu_3$ absorption spectrum to probe its protonation state when bound to MetE. Comparison of free and MetE-bound $CH_3$-$H_4PteGlu_3$ absorbance spectra indicated that the N5 is not protonated in the binary complex. Rapid reaction studies have revealed changes in $CH_3$-$H_4PteGlu_3$ absorbance that are consistent with protonation at N5. These absorbance changes show saturable dependence on both Hcy and $CH_3$-$H_4PteGlu_3$, indicating that protonation of $CH_3$-$H_4PteGlu_3$ occurs upon formation of the ternary complex and prior to methyl transfer. Furthermore, the tetrahydrofolate ($H_4PteGlu_3$) product appears to remain bound to MetE, and in the presence of excess Hcy a MetE·$H_4PteGlu_3$·Hcy mixed ternary complex forms, in which $H_4PteGlu_3$ is protonated.

*I find the reaction catalyzed by cobalamin-dependent methionine synthase improbable, and that catalyzed by cobalamin-independent methionine synthase impossible.*

*−Duilio Arigoni, 1989*

Methionine synthases catalyze the transfer of a methyl group from N5 of methyltetrahydrofolate ($CH_3$-$H_4$folate),[1] a tertiary amine, to the δ-sulfur of homocysteine (Hcy) to form methionine and tetrahydrofolate ($H_4$folate). Tertiary amines are rarely used as methyl donors in biology, because the methyl group is only sluggishly reactive when compared to that of the sulfonium adenosylmethionine (AdoMet), which is the usual biological methyl donor. In cobalamin-dependent methionine synthase (MetH), the "improbable" enzyme, the methyl group is removed from $CH_3$-$H_4$folate by attack of the supernucleophilic cob(I)alamin cofactor and then transferred from the methylcobalamin cofactor to Hcy. However, cobalamin-independent methionine synthase (MetE) lacks any organic cofactor, and the nucleophile is Hcy itself. Hcy has a microscopic p$K_a$ for the thiol of 10 (*1*), so in solution at neutral pH it is present as the thiol rather than the more reactive thiolate (*2*−*4*). We have hypothesized that the strategy to improve the concentration of reactive species would be to shift the p$K_a$ values of the two substrates upon binding to MetE. If the p$K_a$ of Hcy were lowered and that of $CH_3$-$H_4$folate were simultaneously raised on binding to MetE, both substrates would be activated for reaction at neutral pH (Figure 1). Furthermore, this strategy would avoid proton transfer between the substrates in the ternary complex.

Prior studies have established that Hcy is activated by both MetE and MetH using similar strategies. In both cases, the Hcy is coordinated to a zinc ion at the active site of the enzyme (*5*, *6*). In MetH, UV−visible absorbance measurements have established that Hcy binds as a thiolate, with a p$K_a$ that lies at or below 6 (*7*). Thus the role of zinc, which is required for the activity of both enzymes, is to act as a Lewis acid and decrease the p$K_a$ of Hcy on the enzyme. The p$K_a$ of Hcy when bound to zinc in MetE has not been determined. However, consistent with the hypothesis that zinc serves as a Lewis acid, nearly one proton per protein is released upon binding of Hcy to MetE, measured in the presence of a pH indicator at an initial pH of 7.8, suggesting that the p$K_a$ of Hcy is indeed considerably lower than 10 (*7*, *8*).

MetE and MetH have no detectable sequence similarity, and the nature and spacing of the protein residues that bind

† Financial support was received from National Institutes of Health Research Grant GM24908 (R.G.M.) and Michigan NIH Molecular Biophysics Training Grant GM08270 (R.E.T.).

* To whom correspondence should be addressed. E-mail: rmatthew@umich.edu. Fax: (734) 763-6492. Phone: (734) 764-9459.

‡ Department of Biological Chemistry, The University of Michigan.

§ Life Sciences Institute, The University of Michigan.

|| Biophysics Research Division, The University of Michigan.

[1] Abbreviations: $CH_3H_4$folate, methyltetrahydrofolate; $H_4$folate, tetrahydrofolate; AcsE, methyltetrahydrofolate:corrinoid iron/sulfur protein methyltransferase; $CH_3$-$H_4$folate, (6*S*)-*N*5-methyl-5,6,7,8-tetrahydrofolate; $CH_3$-$H_4PteGlu_3$, (6*S*)-*N*5-methyl-5,6,7,8-tetrahydropteroyltriglutamate; $H_4$folate, (6*S*)-5,6,7,8-tetrahydrofolate; $H_4PteGlu_3$, (6*S*)-5,6,7,8-tetrahydropteroyltriglutamate; Hcy, homocysteine; MetE, cobalamin-independent methionine synthase; MetH, cobalamin-dependent methionine synthase; PCA, protocatechuic acid (3,4-dihydroxybenzoate); PCD, protocatechuic acid dioxygenase; $PteGlu_5$, pteroylpentaglutamate.

10.1021/bi060052m CCC: $33.50 
Published on Web 04/05/2006

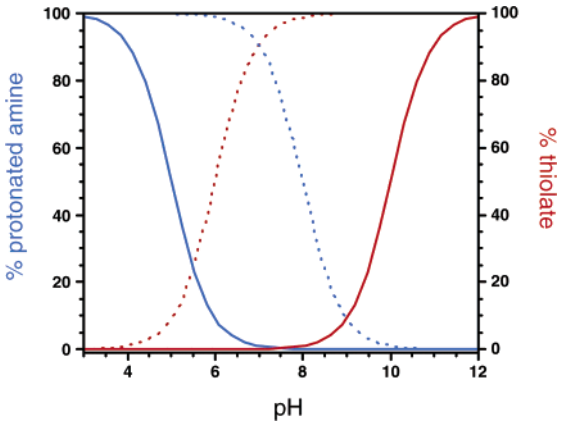


FIGURE 1: A strategy for catalysis by MetE. The p$K_a$ for the N5 of $CH_3$-$H_4$folate is 5 in solution (blue solid line); the microscopic p$K_a$ for deprotonation of the Hcy thiol in solution is 10 (red solid line). Shifting the substrate p$K_a$ values to 8 and 6 (blue and red dotted lines, respectively) would greatly increase the overlap between activated substrates.

the zinc differ. MetE arose from gene duplication and has two homologous domains that both fold into $(\alpha/\beta)_8$ barrels (*9*). The barrels are oriented face-to-face such that the C-termini of the barrel strands point toward each other. Zinc is bound in the C-terminal domain of MetE and is coordinated by protein residues Cys643, Cys726, His641 (*8*), and Glu665 (*E. coli* numbering) (*9*). When Hcy binds to MetE, it coordinates the zinc, causing the metal to move away from Glu665 and toward Hcy (*9*). Even though the zinc/Hcy domains of MetE and MetH have no sequence similarity, they are both $(\alpha/\beta)_8$ barrels with strong structural similarity (*9*). However, MetH has a unique set of zinc ligands: three cysteines and an N/O ligand, presumably a water (*10*). When Hcy coordinates the zinc, the latter ligand is displaced.

The binding of $CH_3$-$H_4$folate to MetE and MetH also is very different. MetH can bind both the monoglutamate and polyglutamate forms of $CH_3$-$H_4$folate, and both can serve as efficient methyl donors (*11*). In contrast, MetE shows an absolute requirement for a polyglutamate derivative (*11*, *12*). Typically, the substrate used is methyltetrahydropteroyltriglutamate ($CH_3$-$H_4$PteGlu$_3$), which is the predominant form in *Escherichia coli* (*13*). A structure of *Thermotoga maritima* MetE shows that $CH_3$-$H_4$PteGlu$_3$ binds between the N- and C-terminal barrels and interacts with a number of conserved residues from both domains (*9*). The N5-methyl points away from the zinc site and is clearly too distant for methyl transfer. These data indicate that the $CH_3$-$H_4$PteGlu$_3$ binary complex is not poised for catalysis and must assume a different conformation for direct methyl transfer to occur. Indeed, a structure of MetE from *Arabidopsis thaliana* was solved with PteGlu$_5$ and methionine bound. In this structure the pterin ring is flipped, such that the N5 is pointing toward the methyl group of methionine (*14*). Such a rotation about the C6−C9 and C9−N10 dihedrals represents one type of conformational change that may take place to allow methyl transfer. It should be noted, however, that the electron density for the pterin is poor in this structure and the ring geometry of PteGlu$_5$ is different from that of reduced folates, which may not be able to adopt this particular conformation.

The p$K_a$ for N5 of $CH_3$-$H_4$PteGlu$_3$ is not perturbed upon binding to MetE in a binary complex (*7*). The UV−visible absorbance of $CH_3$-$H_4$folate changes considerably with pH (*15*) and hydrophobicity (*16*), providing an easily observable signal of the protonation state and environment (Figure 2). The very high protein absorbance limits absorbance measurements to wavelengths above ~307 nm (vertical red line in Figure 2a). This region of the spectrum of the protonated and unprotonated species does not dramatically change shape and differs largely in the magnitude of the extinction coefficients. However, these species can be distinguished on the basis of their characteristic difference spectra. For instance, when the spectrum of $CH_3$-$H_4$folate at pH 7 is subtracted from that of $CH_3$-$H_4$folate at pH 3, the positive difference absorbance below 270−280 nm and negative difference absorbance above 270−280 nm is characteristic of $CH_3$-$H_4$folate protonation (Figure 2a). The difference spectrum associated with binding of $CH_3$-$H_4$PteGlu$_3$ to MetE does not resemble the difference spectrum for protonation of $CH_3$-$H_4$folate in solution (Figure 2b) (*7*). Instead, the difference spectrum associated with formation of the MetE·$CH_3$-$H_4$PteGlu$_3$ binary complex is very similar to that for introducing aqueous $CH_3$-$H_4$PteGlu$_3$ into 80% acetonitrile at neutral pH, suggesting that the $CH_3$-$H_4$PteGlu$_3$ is transferred to a hydrophobic environment on binding to the protein. Additionally, the $K_d$ for binding of the $CH_3$-$H_4$PteGlu$_3$ is invariant between pH 5.5 and pH 8.5, indicating that binary complex formation does not involve either proton uptake or release (*7*).

The spectral changes seen when $CH_3$-$H_4$folate binds MetH are similar to those seen on its binding to MetE, indicating that the environment is hydrophobic and that the $CH_3$-$H_4$folate N5 is not protonated in the MetH binary complex (*16*). In MetH, $CH_3$-$H_4$folate binds in an $(\alpha/\beta)_8$ barrel which forms a separate domain of the protein (*17*). pH−rate profiles of MetH enzyme activity suggest that protonation occurs only in a ternary complex of enzyme, $CH_3$-$H_4$folate, and cob(I)alamin (*7*), in which the cobalamin-binding module of MetH is positioned vis-à-vis the folate-binding barrel. These experiments measured the rate of methyl transfer to exogenous cob(I)alamin from $CH_3$-$H_4$folate bound to a fragment of MetH containing only the folate- and Hcy-binding barrels. This reaction exhibits Theorell−Chance kinetics, in which the ternary complex does not accumulate, so that absorbance measurements of this ternary complex are not possible.

In this contribution, we have taken advantage of the sensitivity of the UV−visible spectra of reduced folates to protonation at N5 and the lack of protein and Hcy absorbance above ~300 nm to monitor the chemical state of the substrate during catalysis. This study of $CH_3$-$H_4$PteGlu$_3$ activation is unique because MetE is the only $CH_3$-$H_4$folate-dependent enzyme that does not catalyze methyl transfer to a corrinoid or cobalamin cofactor, both of which absorb strongly in the UV and visible ranges.

Here we present evidence that $CH_3$-$H_4$PteGlu$_3$ is activated for methyl transfer by protonation of N5 and that the protonation of $CH_3$-$H_4$PteGlu$_3$ requires formation of a ternary complex with both substrates bound to MetE. We provide kinetic evidence that this protonation occurs before methyl transfer. We further demonstrate that the product $H_4$PteGlu$_3$ can also bind MetE in a complex with Hcy and is protonated in this mixed product/substrate ternary complex.

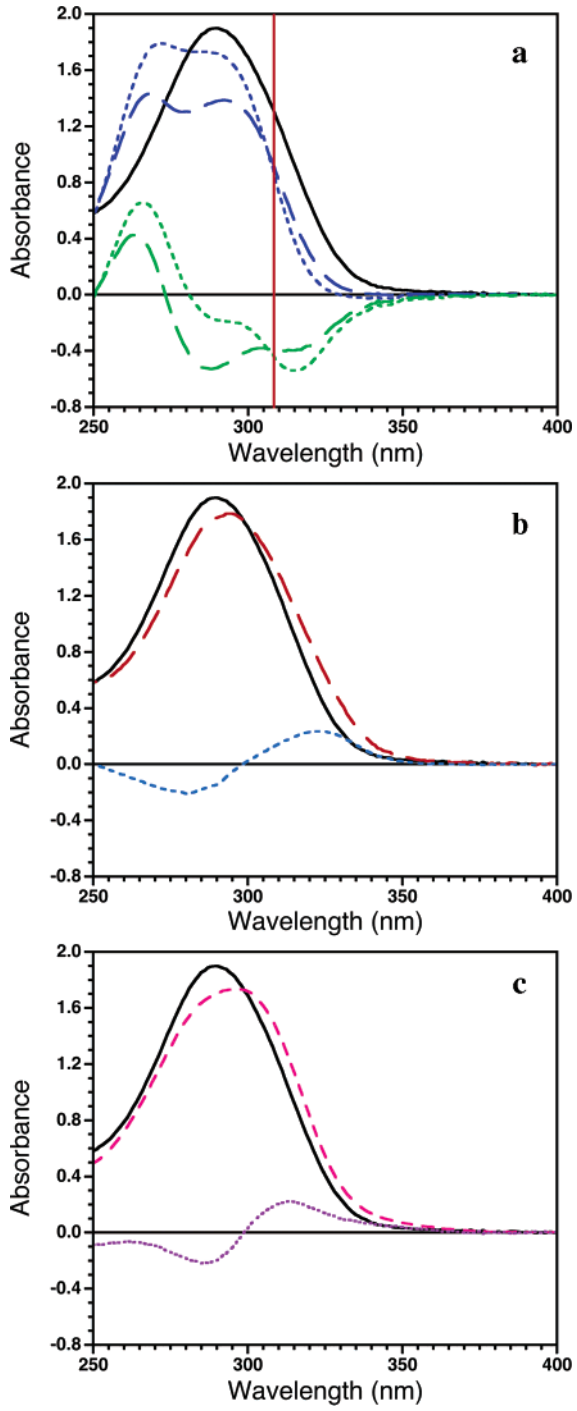


FIGURE 2: Absorbance spectra of reduced folates as a function of protonation state and hydrophobicity. All spectra are normalized to 60 $\mu$M folate. (a) $CH_3$-$H_4$folate at pH 7.2 (solid black line) has a single maximum at 290 nm. When $CH_3$-$H_4$folate is protonated (pH 3 aqueous solution, dashed blue line; pH 3 in 80% acetonitrile, dotted blue line), it gains a second maximum at shorter wavelength. The difference spectra of the protonated $CH_3$-$H_4$folate species minus $CH_3$-$H_4$folate at pH 7.2 each have a characteristic trough beyond 270−280 nm (aqueous solution, dashed green line; 80% acetonitrile, dotted green line). (b) $CH_3$-$H_4PteGlu_3$ bound to MetE at pH 7.2 (dashed red line) is red-shifted with respect to free $CH_3$-$H_4PteGlu_3$ (solid black line). The difference spectrum (dotted blue line) was constructed by subtracting the spectra of free $CH_3$-$H_4PteGlu_3$ and free MetE from the spectrum of the MetE·$CH_3$-$H_4PteGlu_3$ binary complex. (c) $H_4$folate at pH 7.2 (dashed pink line) is red-shifted with respect to $CH_3$-$H_4$folate (black line). The difference spectrum (dotted purple line) was constructed by subtracting the $CH_3$-$H_4$-folate spectrum at pH 7.2 from $H_4$folate at pH 7.2.

## MATERIALS AND METHODS

*Reagents.* Dithiothreitol was purchased from Bio-Rad (Hercules, CA). (6*S*)-$CH_3$-$H_4PteGlu_1$ and (6*S*)-$H_4PteGlu_1$ were a gift from Eprova (Schaffhausen, Switzerland). Potassium phosphate and other buffer components were purchased from Fisher Scientific (Fair Lawn, NJ). Protocatechuic acid dioxygenase (PCD) was a generous gift from David P. Ballou. Hcy thiolactone and all other materials were obtained from Sigma (St. Louis, MO). See the accompanying paper (*35*) for expression and purification of MetE, as well as the synthesis of (6*S*)-$CH_3$-$H_4PteGlu_3$ and Hcy.

*Absorbance Spectra of Free Folate Species.* Spectra of folates in solution were obtained using either an HP 845x diode array or a Cary 50 Bio UV−visible spectrophotometer. Spectra of $CH_3$-$H_4PteGlu_1$ in AMT buffer with and without 80% acetonitrile were obtained previously (*7*, *16*). Stocks (~1 mM) of $H_4PteGlu_1$ were made fresh on the day of use in water with 10 mM dithiothreitol, and aliquots from the stock were diluted (100-fold) into various buffers to obtain spectra. All buffers were bubbled with oxygen-scrubbed argon for at least 10 min. The spectrum of $H_4PteGlu_1$ in aqueous solution was obtained as previously described (*15*) in 70 mM sodium formate, 70 mM sodium acetate, and 70 mM potassium phosphate buffer, brought to either pH 7.2 or pH 3.0 with hydrochloric acid and approximately 1 M ionic strength with sodium chloride. The spectrum of protonated $H_4PteGlu_1$ in a hydrophobic solution was obtained in 80% acetonitrile and 20% water, brought to pH 3.0 with phosphoric acid.

*Stopped-Flow Measurements.* Rapid reaction studies were carried out in a Hi-Tech Scientific model SF-61DX2 stopped-flow spectrophotometer (TgK Scientific Ltd., Bradford on Avon, Wiltshire, U.K.) in single mixing mode, using a deuterium light source for single wavelength detection or a tungsten light source for diode array detection. All stopped-flow experiments were performed under anaerobic conditions. The instrument was flushed with 100 mM potassium phosphate, pH 7.2, containing ~0.1 unit/mL protocatechuate dioxygenase (PCD) and 1 mM protocatechuate [PCA (3,4-dihydroxybenzoate)] and allowed to stand overnight (*18*). PCA and PCD were flushed from the system with MetE assay buffer (50 mM Tris, 10 mM potassium phosphate, pH 7.2, 100 $\mu$M $MgSO_4$, 1 mM dithiothreitol), which had been bubbled for at least 10 min with oxygen-free argon. Enzyme and substrate solutions were made anaerobic in glass tonometers by cycling quickly between vacuum and oxygen-scrubbed argon five times, followed by 5 min of equilibration with argon at room temperature; this procedure was repeated ten times. All measurements were performed at 25 °C in MetE assay buffer.

Apparent rate constants were calculated from exponential fits of single wavelength absorbance traces in Kaleidagraph 3.6 (Synergy Software, Reading, PA) using eq 1 (*19*).

$$A = A_\infty + \Delta A_1 e^{-k_1 t} + \Delta A_2 e^{-k_2 t} + \ldots \quad (1)$$

Typically, amplitudes and rate constants from two to six shots were averaged, and the error was calculated as the standard deviation from the mean. The sum of the amplitudes of the first two phases were fit to eq 2 (*20*).

$$\Delta A = \frac{\Delta A_{max}}{2[EA]_t}\{([EA]_t + [B]_t + K_d) - \sqrt{([EA]_t + [B]_t + K_d)^2 - 4[EA]_t[B]_t}\} \quad (2)$$

Spectra of intermediates were calculated from global fits of diode array data using SpecFit/32, version 3.0 (Spectrum Software Associates, Claix, France). The refined rate constants and amplitudes from the fit were used to calculate the spectrum of each reaction intermediate (at 100%) in SpecFit. The spectrum of each intermediate was determined as an average from multiple shots taken under the same conditions, unless noted.

*E·H4PteGlu3 Spectral Titrations*. All spectra were obtained using an HP 845x diode array spectrophotometer. A solution of MetE and $CH_3$-$H_4$PteGlu$_3$ in MetE assay buffer was made anaerobic via a side port in a closed cuvette by the method described above for stopped-flow tonometers. A solution of 10 mM Hcy was bubbled with oxygen-free argon for at least 20 min. One equivalent of Hcy was introduced through a PTFE/silicone septum (Fisher Scientific), held by a screw cap at the top of the cuvette, into the solution containing MetE and $CH_3$-$H_4$PteGlu$_3$ using a 100 $\mu$L Hamilton syringe equipped with an aliquoter (2 $\mu$L/aliquot). The reaction was allowed to proceed to completion (as determined by constant absorption spectra) after which the rest of the Hcy was added in 2−6 $\mu$L aliquots and a spectrum was obtained after each addition.

## RESULTS

*Observation of a Pre-Steady-State Ternary MetE·CH3-H4PteGlu3·Hcy Complex in Which CH3-H4PteGlu3 Is Protonated*. A binary complex of MetE and $CH_3$-$H_4$PteGlu$_3$ was mixed with free Hcy, resulting in a rapid decrease in absorbance at 324 nm, followed by a rise (Figure 3a). The initial decrease in absorbance observed in the stopped-flow spectrophotometer under single turnover conditions (equimolar enzyme and substrates or limiting substrate) fit best to two phases. The spectra associated with each phase were monitored in a stopped-flow spectrophotometer with a diode array detector (Figure 4a). To better distinguish the spectral changes that occur during the reaction, the first spectrum (taken at 3 ms) was subtracted from all subsequent spectra. The difference spectra associated with the first two phases bear a strong resemblance to the difference spectrum of $CH_3$-$H_4$PteGlu$_3$ protonated in a hydrophobic environment (Figure 2a) minus unprotonated $CH_3$-$H_4$PteGlu$_3$ bound in the MetE binary complex (Figure 2b). Since the MetE·$CH_3$-$H_4$PteGlu$_3$ binary complex is formed before the reaction begins, its spectrum was used as the initial spectrum to construct this model difference spectrum for protonation (dotted line in Figure 4), as opposed to the difference spectrum for protonation shown in Figure 2a, in which the spectrum of free unprotonated $CH_3$-$H_4$folate was subtracted from that of protonated $CH_3$-$H_4$folate in 80% acetonitrile. The difference spectra obtained in the first 220 ms of the MetE reaction appear to be red shifted by ~3 nm with respect to the difference spectrum of protonated $CH_3$-$H_4$PteGlu$_3$ in 80% acetonitrile at pH 3. These observations may reflect the difference in dielectric constant between 80% acetonitrile and the active site of MetE. The total amplitude of the absorbance change appears to be smaller in the diode array than in experiments performed at a single wavelength due to a longer dead time (2.99 ms) in the diode array setup than the photomultiplier setup used for single wavelength measurements (1.5 ms dead time).

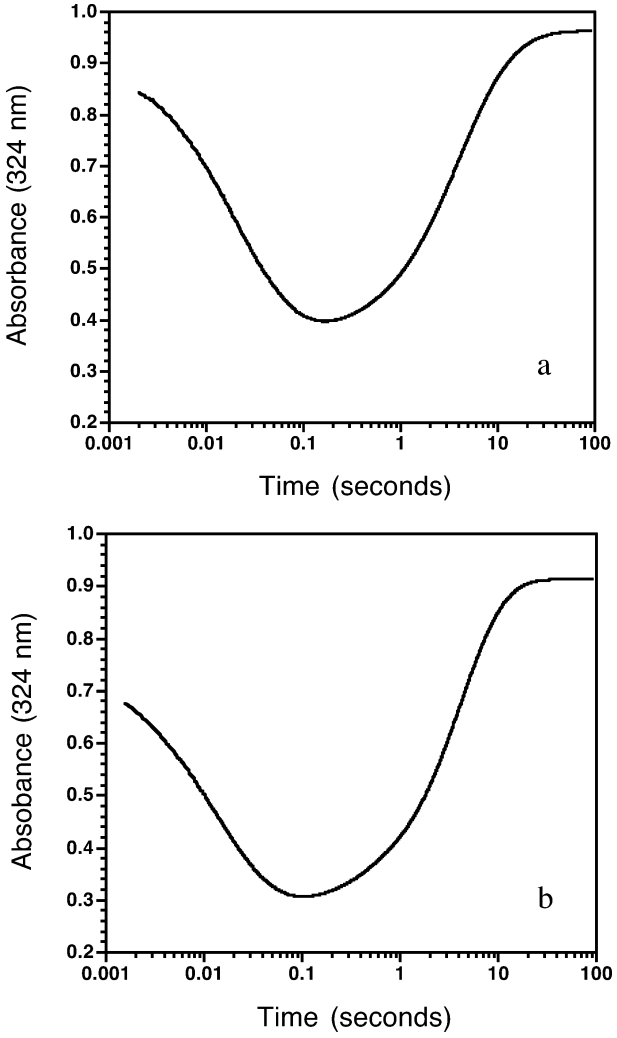


FIGURE 3: Traces of absorbance changes at 324 nm during the MetE reaction. (a) MetE and $CH_3$-$H_4$PteGlu$_3$ (60 $\mu$M each) were preincubated and then mixed with Hcy (60 $\mu$M) and monitored in a stopped-flow spectrophotometer. (b) MetE and Hcy (60 $\mu$M each) were preincubated and then reacted with $CH_3$-$H_4$PteGlu$_3$ (60 $\mu$M) in a stopped-flow spectrophotometer.

When the order of the reaction was switched and the same concentration of the MetE·Hcy binary complex was reacted with $CH_3$-$H_4$PteGlu$_3$, the absorbance changes were very similar (Figure 3b). Two phases of decreasing absorbance were followed by an increase in absorbance at 324 nm. The difference spectra from the first two phases have the same shape as those obtained from the reaction in which substrates were added in the opposite order (Figure 4b). However, the rate constant for the first phase is faster when the reaction is initiated by adding $CH_3$-$H_4$PteGlu$_3$, so that the apparent absorbance change reaches its minimum faster (120 ms) and is smaller because more of the decrease is missed in the instrument dead time.

The amplitudes of the absorbance decrease in each of the two fast phases were dependent on $CH_3$-$H_4$PteGlu$_3$ concentration (data not shown), and the sum of these two amplitudes (total absorption decrease) was shown to have a stoichiometric dependence on all three reaction compo-

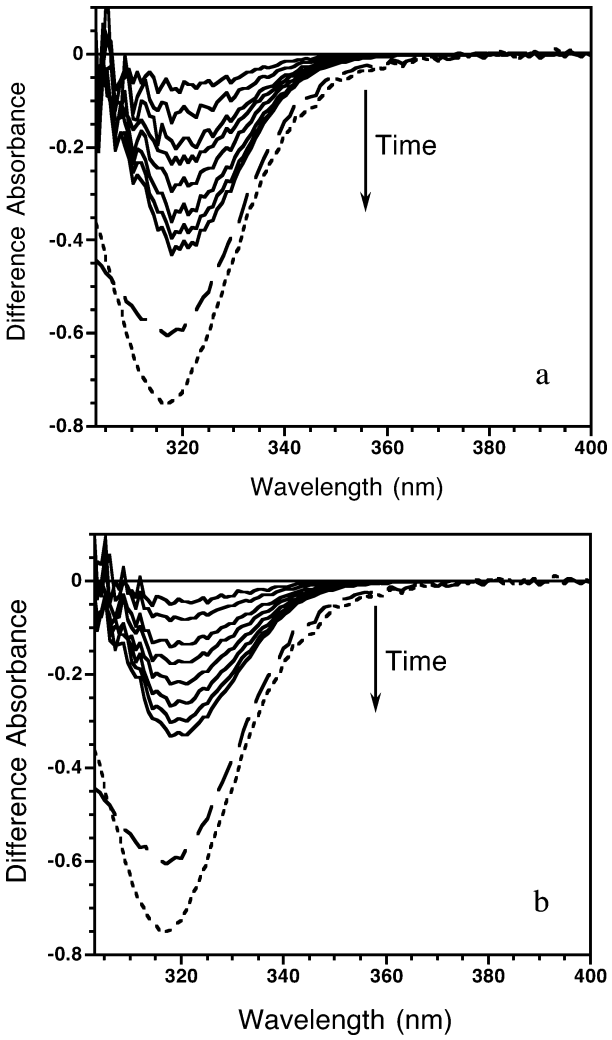


FIGURE 4: Difference spectra associated with the first two phases of the MetE reaction. Difference spectra were obtained by subtracting the first spectrum (obtained at 2.99 ms) from each subsequent spectrum during the reaction. The dashed lines show the difference spectrum of $CH_3$-$H_4$folate (60 $\mu$M) in aqueous solution at pH 3 minus the spectrum of the MetE·$CH_3$-$H_4$$PteGlu_3$ binary complex. The dotted lines show the difference spectrum of $CH_3$-$H_4$folate protonated in 80% acetonitrile minus the spectrum of MetE·$CH_3$-$H_4$$PteGlu_3$. (a) MetE and $CH_3$-$H_4$$PteGlu_3$ (60 $\mu$M each) were preincubated and then mixed with Hcy (60 $\mu$M) and monitored in a stopped-flow spectrophotometer; the first 220 ms of reaction are shown. (b) MetE and Hcy (60 $\mu$M each) were preincubated and then mixed with $CH_3$-$H_4$$PteGlu_3$ (60 $\mu$M) and monitored in a stopped-flow spectrophotometer; the first 120 ms of reaction are shown.

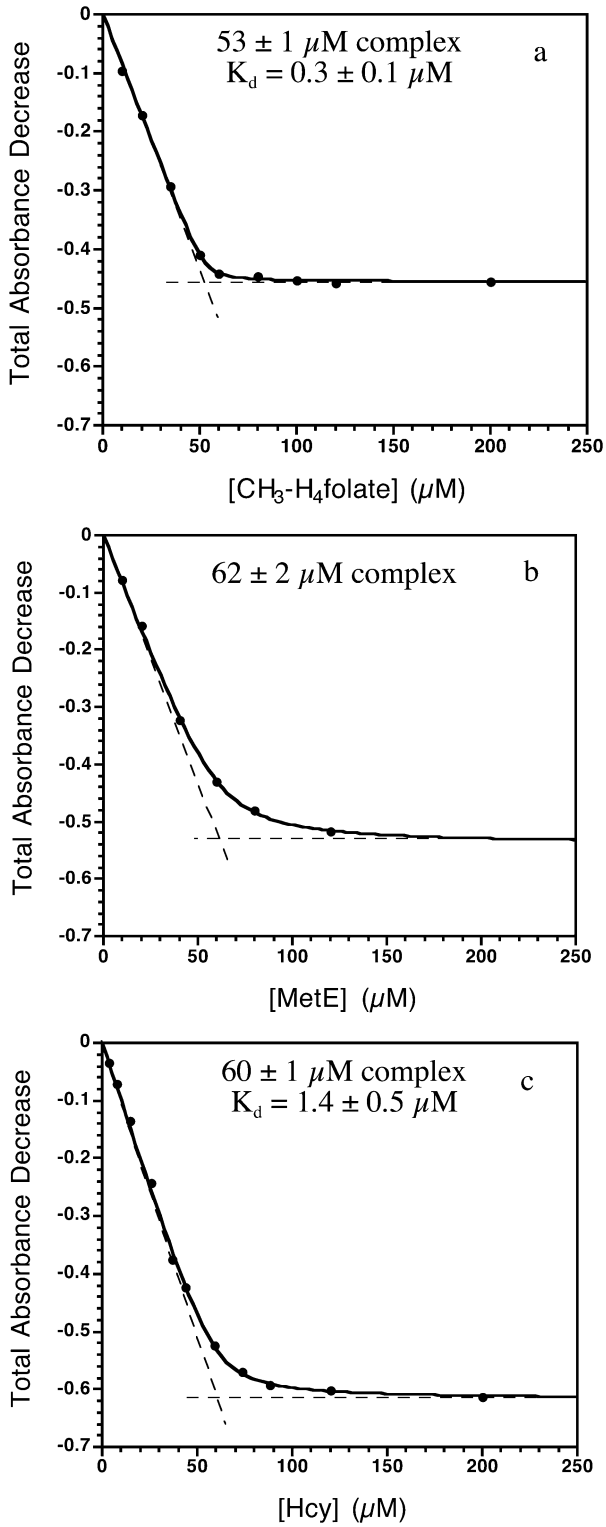


FIGURE 5: Dependence of the absorbance decrease at 324 nm on Hcy, MetE, and $CH_3$-$H_4$$PteGlu_3$. The absorbance decrease observed in the stopped-flow spectrophotometer was fit to two exponentials, and the amplitudes of each phase were added together. (a) MetE and Hcy (60 $\mu$M each) were reacted with $CH_3$-$H_4$$PteGlu_3$ (10−200 $\mu$M), (b) MetE (10−120 $\mu$M) and Hcy (60 $\mu$M) were reacted with $CH_3$-$H_4$$PteGlu_3$ (60 $\mu$M), and (c) MetE and $CH_3$-$H_4$$PteGlu_3$ (60 $\mu$M each) were reacted with Hcy (3.6−200 $\mu$M).

nents: $CH_3$-$H_4$$PteGlu_3$, MetE, and Hcy (Figure 5). These observations suggest that the decrease in absorbance at 324 nm requires formation of a MetE·$CH_3$-$H_4$$PteGlu_3$·Hcy ternary complex.

The total absorption decrease at 324 nm reaches a maximum of 0.617 ± 0.008 (Figure 5c). To take into account the 3 nm shift of the absorbance minimum between the model difference spectrum for protonation (dotted lines in Figure 4) and that observed in the stopped flow (solid lines in Figure 4), 324 nm was compared to 321 nm from the model difference spectrum for protonation, with the assumption that the spectra shift but the extinction coefficients do not change. It should be noted that these wavelengths are near, but not at, the minima in their respective difference absorbance spectra. The absorbance decrease for transferring 60 $\mu$M $CH_3$-$H_4$$PteGlu_3$ from the MetE binary complex into 80% acetonitrile, pH 3 at 321 nm, is 0.7. Therefore, the changes in stopped-flow absorbance are consistent with formation of

a ternary complex in which $CH_3$-$H_4$PteGlu$_3$ is almost completely protonated.

The total absorbance decrease was consistently lower when MetE was preincubated with Hcy (Figure 5a,b) instead of $CH_3$-$H_4$PteGlu$_3$ (Figure 5c) under the same conditions, probably because the ternary complex is not fully saturated at 60 $\mu$M Hcy, and thus the greatest absorbance decrease that can be expected at this Hcy concentration is about 0.52, consistent with the 60 $\mu$M data point in Figure 5c. Additionally, a slightly lower initial concentration of the E·Hcy binary complex is suggested by the saturation point in Figure 5a and would produce a smaller absorbance decrease.

Spectra of reaction intermediates were determined by fitting the spectra collected during the reaction to a set of three consecutive exponentials (A → B → C → D; fits to parallel exponentials yielded extinction coefficients that were either negative or too high to be believable). When the MetE·Hcy binary complex was reacted with $CH_3$-$H_4$PteGlu$_3$, the starting spectrum from this fit did not agree with the sum of the spectra of the reactants, MetE·Hcy and $CH_3$-$H_4$PteGlu$_3$ (Figure 6a). Instead, the spectrum of the first species observed after the instrument dead time (intermediate A) closely resembled the spectrum of the MetE·$CH_3$-$H_4$PteGlu$_3$ binary complex (shown as a difference spectrum in Figure 6b), suggesting that $CH_3$-$H_4$PteGlu$_3$ binds in the instrument dead time forming a ternary complex with absorbance properties similar to those observed when Hcy is not present. In contrast, when the MetE·$CH_3$-$H_4$PteGlu$_3$ binary complex was reacted with Hcy, the starting spectrum calculated from the fit (intermediate A) and the actual initial spectrum were essentially the same (data not shown). Subtraction of the initial MetE·$CH_3$-$H_4$PteGlu$_3$ binary complex spectrum from the spectra of the next two intermediates yielded difference spectra that were very similar to those expected for protonation of $CH_3$-$H_4$PteGlu$_3$ in a hydrophobic environment (Figure 7). While the shapes of the intermediate spectra are alike, the amplitude of intermediate B is smaller, and it is not until the formation of intermediate C that the "full" magnitude of the absorbance decrease is observed.

*Observation of a Phase Corresponding to Methyl Transfer.* After formation of the ternary complex and the initial decrease in absorbance, a phase of increasing absorbance was observed in the stopped flow (Figure 3). This phase is likely to represent the chemical step, since conversion of $CH_3$-$H_4$PteGlu$_3$ to $H_4$PteGlu$_3$ is expected to lead to an absorbance increase at 324 nm (Figure 2c). The rate constant for this phase is substrate-independent and corresponds with the $k_{chem}$ of 0.25 ± 0.09 s$^{-1}$ that was determined directly by monitoring the irreversible transfer of the radiolabel from [*methyl*-$^{14}$C]$CH_3$-$H_4$PteGlu$_3$ to form [*methyl*-$^{14}$C]Met [Figure 2 in the accompanying paper (*35*)]. These data together demonstrate that protonation of $CH_3$-$H_4$PteGlu$_3$ occurs in a kinetically competent fashion. However, the final difference spectrum observed in the diode array, intermediate D, did not match that expected for free $H_4$PteGlu$_3$ (Figure 2c). To confirm that this calculated final spectrum was actually the spectrum of the reaction product, equimolar MetE and $CH_3$-$H_4$PteGlu$_3$ were reacted with Hcy in a spectrophotometer; the observed spectrum did indeed agree with the actual and calculated spectra of the product seen in the stopped-flow spectrophotometer when Hcy was the limiting substrate (Figure 8). This difference spectrum is very red shifted with respect to that of $H_4$PteGlu$_3$ in aqueous solution, reminiscent of the red shift observed with increasing hydrophobicity of the $CH_3$-$H_4$PteGlu$_3$ environment both in solution and upon binding to MetE (*7*, *16*). It is therefore likely that the $H_4$-PteGlu$_3$ product remains bound on the enzyme after a single turnover, though perhaps only at the high concentrations of MetE and $H_4$PteGlu$_3$ employed in this experiment.

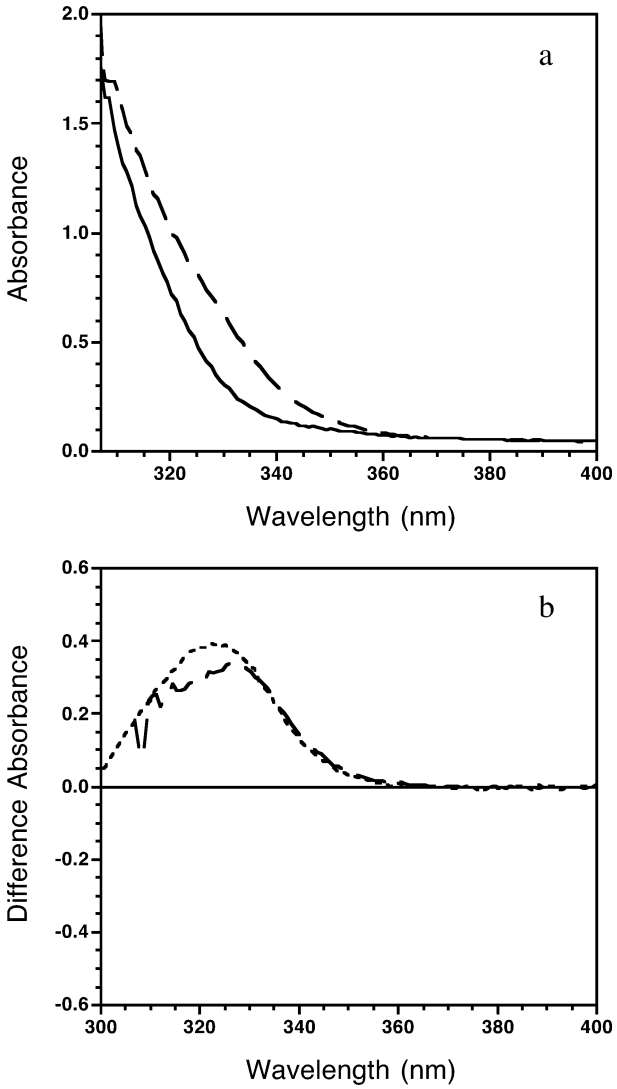


FIGURE 6: Formation of the ternary complex when $CH_3$-$H_4$PteGlu$_3$ is mixed with MetE·Hcy. (a) MetE and Hcy (100 $\mu$M each) were reacted with $CH_3$-$H_4$PteGlu$_3$ (100 $\mu$M) in a stopped-flow spectrophotometer equipped with a diode array detector. The solid line shows the initial spectrum, calculated as the sum of the MetE·Hcy and free $CH_3$-$H_4$PteGlu$_3$ spectra. The dashed line shows the first spectrum observed in the stopped-flow spectrophotometer after the 3 ms dead time (intermediate A). (b) The dashed line is the difference of the initial spectrum subtracted from the spectrum of intermediate A. The dotted line is the experimentally obtained difference spectrum of free MetE and free $CH_3$-$H_4$PteGlu$_3$ spectra subtracted from the MetE·$CH_3$-$H_4$PteGlu$_3$ binary complex spectrum (*7*), normalized to 100 $\mu$M.

*Observation of a Ternary MetE·$H_4$PteGlu$_3$·Hcy Complex.* When the MetE·$CH_3$-$H_4$PteGlu$_3$ binary complex is mixed with more than 2 equiv of Hcy, another level of complexity is observed in the stopped-flow traces. At least one extra phase is observed after the initial absorbance decreases (Figure 9), with a rate constant slightly greater than $k_{chem}$. Additionally, the amplitude of the phase corresponding to

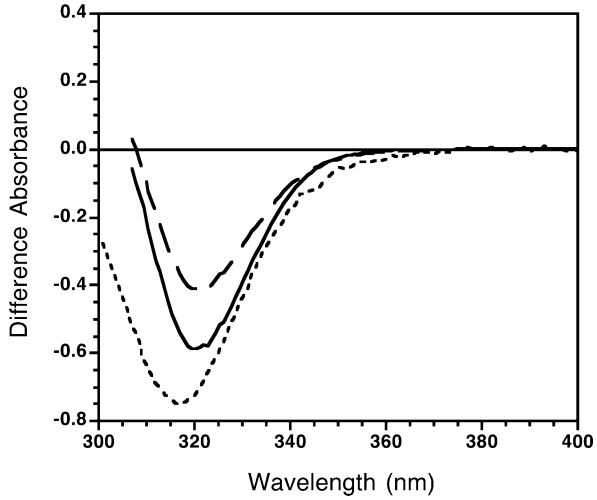


FIGURE 7: Difference spectra of reaction intermediates B and C. Difference spectra of intermediates B (dashed line) and C (solid line) were obtained by subtracting the starting spectrum of MetE·$CH_3$-$H_4$PteGlu$_3$ (60 $\mu$M) from the spectrum of each subsequent reaction intermediate. The difference spectrum for protonation of $CH_3$-$H_4$PteGlu$_3$ in a hydrophobic environment (dotted line) was obtained by subtracting the MetE·$CH_3$-$H_4$PteGlu$_3$ binary complex spectrum from the solution spectrum of $CH_3$-$H_4$PteGlu$_3$ taken at pH 3 in 80% acetonitrile.

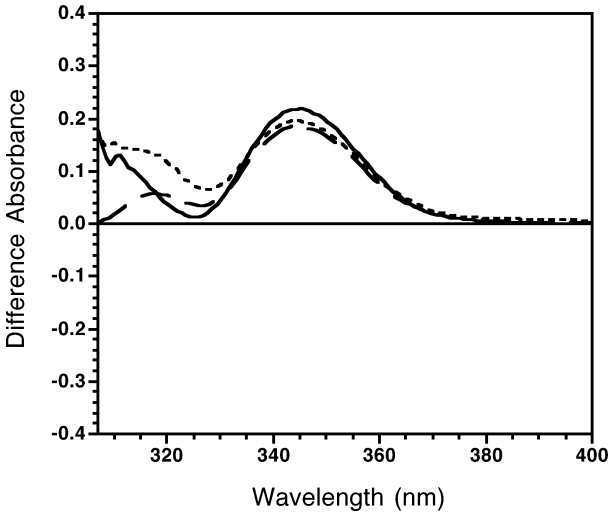


FIGURE 8: Difference spectra for product formation during a single turnover of MetE and for formation of intermediate D. MetE and $CH_3$-$H_4$PteGlu$_3$ (60 $\mu$M each) were titrated with 2 equiv of Hcy (the dashed line shows the difference spectrum obtained after addition of 1 equiv; the dotted line is after addition of 2 equiv) at which point the absorbance at 345 nm reached a maximum. The spectrum of the initial MetE·$CH_3$-$H_4$PteGlu$_3$ binary complex was subtracted from the subsequent spectra to obtain difference spectra. The difference spectrum for formation of intermediate D (solid line) was obtained by subtracting the initial spectrum of the MetE·$CH_3$-$H_4$PteGlu$_3$ binary complex.

the chemical step decreases progressively as the concentration of Hcy is raised. However, essentially complete transfer of a radiolabeled methyl group was observed at similarly high concentrations of Hcy in the course of determining $k_{chem}$ [see accompanying paper (*35*)].

The spectrum of an additional species, intermediate E, was determined assuming a four-step consecutive mechanism (A → B → C → D → E) and resembled protonated tetrahydrofolate (Figure 10a,b). Since this complexity was dependent on the presence of excess Hcy, we hypothesized that Hcy

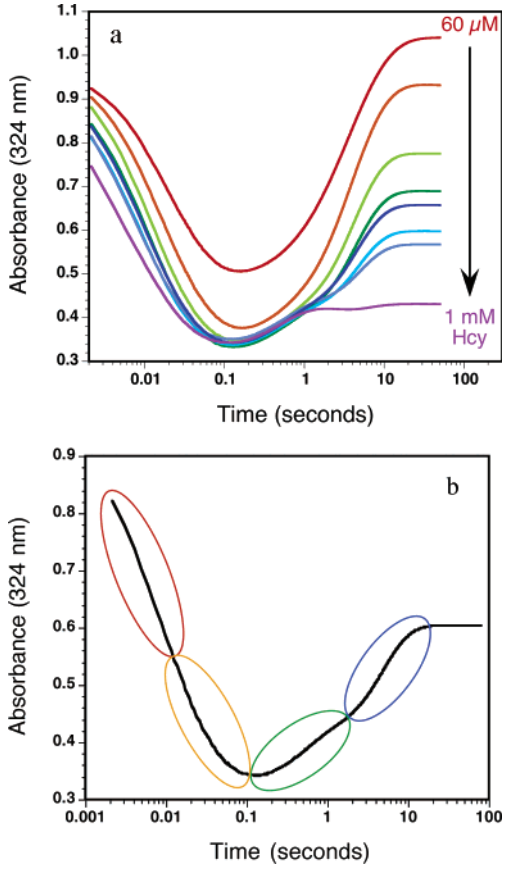


FIGURE 9: Variation of the final absorbance at 324 nm with the concentration of Hcy. (a) MetE (60 $\mu$M) was preincubated with $CH_3$-$H_4$PteGlu$_3$ (60 $\mu$M) before mixing with Hcy (60 $\mu$M−1 mM) and monitoring the absorbance change in the stopped-flow spectrophotometer at 324 nm. (b) Absorbance changes at 324 nm associated with reaction of MetE and $CH_3$-$H_4$PteGlu$_3$ (60 $\mu$M each) with 300 $\mu$M Hcy. The data were fit to four parallel exponentials, as indicated by the colored circles: $k_{obs1}$ = 126 $s^{-1}$ (red circle), $k_{obs2}$ = 26 $s^{-1}$ (orange circle), $k_{obs3}$ = 4.8 $s^{-1}$ (green circle), and $k_{obs4}$ = 0.23 $s^{-1}$ (blue circle).

was binding to the enzyme after methyl transfer, to form a MetE·$H_4$PteGlu$_3$·Hcy ternary complex. To explore this possibility, $H_4$PteGlu$_3$ was formed by adding aliquots of Hcy to a cuvette containing equimolar MetE and $CH_3$-$H_4$PteGlu$_3$ (Figure 8). Further titration of this MetE/product solution with Hcy caused a change in absorbance, which mirrored that observed in stopped-flow experiments performed at high Hcy concentrations (Figure 10a). The initial MetE·$CH_3$-$H_4$-PteGlu$_3$ spectrum was subtracted from the subsequent spectra obtained with increasing concentrations of Hcy. The difference spectra associated with the Hcy titration and with formation of intermediate E most resemble difference spectra for conversion of MetE-bound $CH_3$-$H_4$PteGlu$_3$ to $H_4$PteGlu$_3$ protonated in a hydrophobic environment (Figure 10b). The protonation of $H_4$PteGlu$_3$ in the presence of MetE and Hcy implies that a "mixed" MetE·$H_4$PteGlu$_3$·Hcy ternary complex can be formed that has absorbance properties similar to those of the substrate ternary complex. The absorbance at 324 nm was plotted against the concentration of Hcy, and the data were fit to eq 2, resulting in a $K_d$ of 34 ± 5 $\mu$M for Hcy binding to the E·$H_4$PteGlu$_3$ complex (Figure 10c). Since formation of the mixed ternary complex occurs with slightly faster kinetics than methyl transfer, the appearance of this complex largely masks the absorbance change accompanying

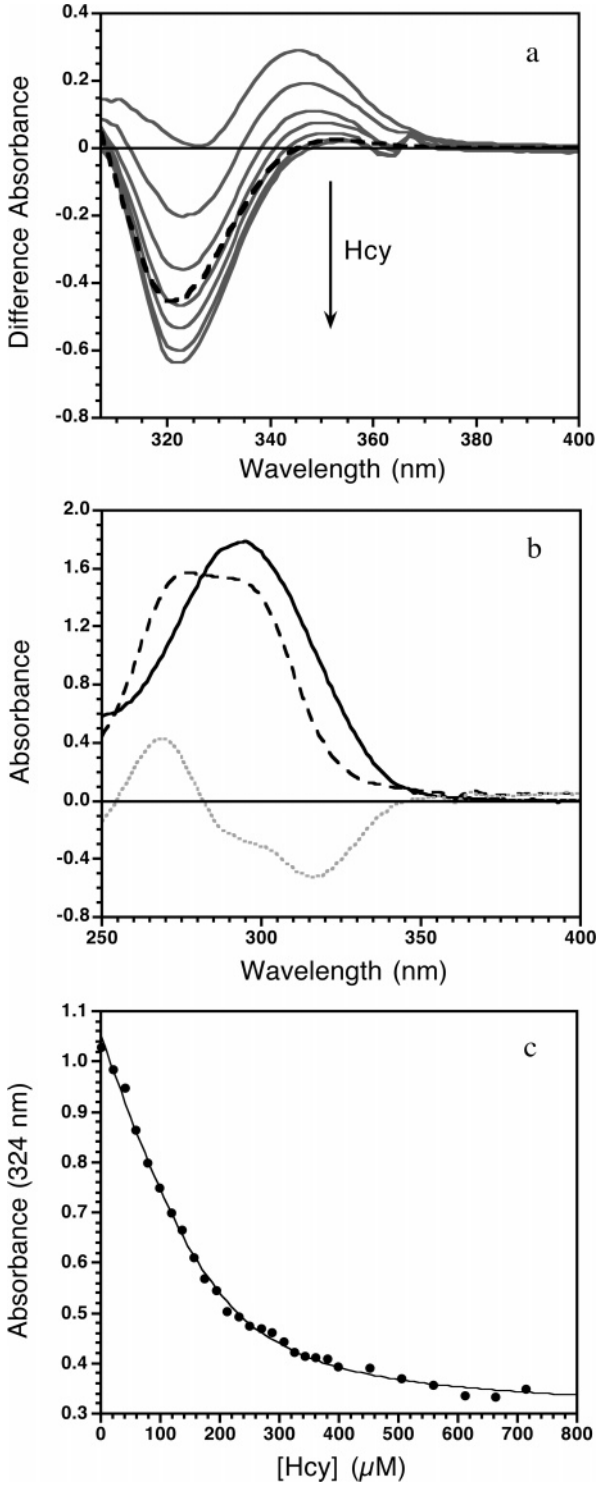


FIGURE 10: Formation of a MetE·$H_4$PteGlu$_3$·Hcy ternary complex. (a) The products from a single turnover of MetE (60 $\mu$M) were titrated with Hcy (final concentration = 713 $\mu$M). The spectrum of the initial MetE·$CH_3$-$H_4$PteGlu$_3$ binary complex was subtracted from the subsequent spectra to obtain difference spectra (solid gray lines). The difference spectrum associated with formation of intermediate E (dashed black line) was obtained by subtracting out the initial spectrum of the MetE·$CH_3$-$H_4$PteGlu$_3$ binary complex. (b) The spectrum of the MetE·$CH_3$-$H_4$folate binary complex (60 $\mu$M) at pH 7.2 (solid black line) was subtracted from the spectrum of $H_4$folate (60 $\mu$M) at pH 3 in 80% acetonitrile (dashed black line) to obtain the difference spectrum (dotted gray line) associated with protonation of $H_4$folate in a hydrophobic environment. (c) The decreasing absorbance at 324 nm due to Hcy binding was fit to eq 2, from which a $K_d$ of 34 ± 5 $\mu$M was obtained.

methyl transfer. Scheme 1 shows the complete set of steps in the MetE reaction, starting with the MetE·Hcy or MetE·$CH_3$-$H_4$PteGlu$_3$ binary complex and including the formation of the mixed ternary E·Hcy·$H_4$PteGlu$_3$ complex.

It is not yet clear whether high concentrations of Hcy cause inhibition of turnover under physiological conditions due to the formation of a mixed ternary complex. No inhibition by Hcy has been observed under steady-state conditions, perhaps because the concentration of MetE is very low (~250 nM), and initial rates are measured, such that very little $H_4$PteGlu$_3$ is formed during the course of our measurements. However, as discussed in the accompanying paper (*35*), the $k_{cat}$ for MetE is about 2-fold lower than for $k_{chem}$, suggesting that release of products from the MetE·$H_4$PteGlu$_3$·Met ternary complex may be partially rate limiting.

Since the p$K_a$ values for N5 of $H_4$folate and $CH_3$-$H_4$folate are very close, 4.82 and 5.1, respectively (*15*, *16*), it is not unreasonable that their p$K_a$ values would be affected similarly by a particular environment. The mixed ternary complex appears to be relatively stable and presents a unique opportunity to further investigate a MetE ternary complex by methods that cannot be used with the catalytically competent ternary complex. Not only can the protonation state of $H_4$PteGlu$_3$ be probed, but more information about the structural differences between the binary and ternary complexes may be gained.

## DISCUSSION

*Model Studies of Methyl Transfer Reactions.* The methyl transfer reaction catalyzed by MetE is chemically challenging. Model studies of nucleophilic methyl transfer reactions have demonstrated that the reaction rate is influenced by the reactivity of both the nucleophile and the leaving group (*21*). In these studies, which employed (2-aminocyclopentyl)ethyl onium salts with a *p*-nitrophenyl leaving group, the reactivity of an ammonium salt was shown to be ~100-fold lower than that of the analogous sulfonium compound. This lower reactivity correlated with greater dependence on nucleophilicity, reflected in a Brønsted $\beta$ of ≥0.49, compared to 0.34 for the sulfonium salts. More recent studies have extended the comparison to include the reactivity of protonated tertiary vs quaternary amines (*22*). These studies employed methylammonium and methylsulfonium salts. Measurements of the disproportionation of dimethylamine to mono- and trimethylamine in water under conditions where half of the dimethylamine is protonated showed that the reaction rate is approximately 5-fold slower than the rate of reaction of the same concentration of tetramethylammonium with dimethylamine. The rate of disproportionation of dimethylamine was also dependent on the protonation state of the donor and acceptor amines and was fastest when the pH was equivalent to the p$K_a$ of dimethylamine (*22*) These studies also compared the reactivity of methylsulfonium and methylammonium salts, and for these compounds the reactivity of the sulfonium was about 10000-fold greater than that of methylammonium. Thus, compared to the reactivity of a sulfonium, like AdoMet, as a methyl donor, these studies would predict that a protonated tertiary amine would be between 500- and 50000-fold less reactive. De novo biosynthesis of methyl groups requires a tertiary amine precursor, and the model chemistry indicates that formation of protonated $CH_3$-$H_4$-folate improves the substrate reactivity.

Scheme 1: Schematic Representation of the Steps in the MetE Reaction

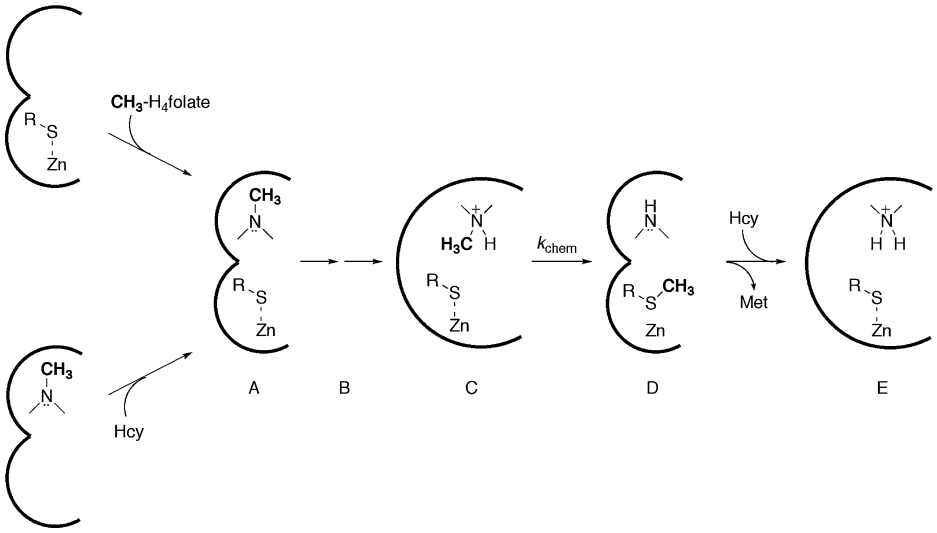


*Factors Leading to the Stabilization of Protonated $CH_3$-$H_4$PteGlu$_3$ in the Ternary Complex.* The experiments reported in this contribution have established that absorbance changes consistent with protonation of $CH_3$-$H_4$PteGlu$_3$ occur only when a ternary MetE·$CH_3$-$H_4$PteGlu$_3$·Hcy complex forms. These changes occur substantially faster than the subsequent transfer of the methyl group from $CH_3$-$H_4$PteGlu$_3$ to Hcy, allowing the accumulation of the activated ternary complex. The maximum observed absorbance decrease associated with formation of the MetE·$CH_3$-$H_4$PteGlu$_3$·Hcy ternary complex (Figure 5c) is approximately 90% of that observed for transfer of 60 $\mu$M $CH_3$-$H_4$folate from the MetE·$CH_3$-$H_4$PteGlu$_3$ binary complex to 80% acetonitrile at pH 3. Assuming that the extinction coefficients are the same for protonated forms of enzyme-bound and free $CH_3$-$H_4$folate, these observations suggest that the p$K_a$ of $CH_3$-$H_4$PteGlu$_3$ in the ternary complex must lie well above pH 7.

The factors responsible for the stabilization of the protonated form of $CH_3$-$H_4$PteGlu$_3$ in the ternary complex remain to be established. The 3 nm red shift associated with the difference spectrum seen on protonation of $CH_3$-$H_4$PteGlu$_3$ when bound to MetE as compared to that observed in acidic acetonitrile suggests that the active site of MetE is more hydrophobic than 80% acetonitrile (dielectric of ~47 at 20 °C) (*23*). Indeed, many studies suggest that typical protein active sites are characterized by low dielectric constants (dielectric of ~4) (*24*, *25*). Such a low dielectric constant would be expected to disfavor protonation of $CH_3$-$H_4$PteGlu$_3$ in the binary complex, provided that the positive charge on N5 remains uncompensated by a negative charge provided by the protein. Indeed, the structure of the binary MetE·$CH_3$-$H_4$PteGlu$_3$ does not reveal any mechanism for stabilizing a positive charge on N5 (*9*). However, the interaction between paired positive and negative charges in an environment of low dielectric is extremely favorable (*26*). Bringing the partial negative charge on the sulfur of homocysteine in proximity to N5 of $CH_3$-$H_4$PteGlu$_3$ would be expected to favor protonation of $CH_3$-$H_4$PteGlu$_3$ when the ternary complex forms.

The structural characterization of MetE indicates that the initial binary MetE·$CH_3$-$H_4$PteGlu$_3$ complex has the folate oriented in a nonproductive binding mode, with the N5-methyl group pointing away from the homocysteine binding site and one face of the folate exposed to solvent. As discussed in the introduction, the folate must reorient in the ternary complex to allow methyl transfer. This reorientation may account for one of the two phases associated with formation of the fully protonated ternary complex, although we do not yet know which phase this might be.

An additional factor that could potentially contribute to stabilization of $CH_3$-$H_4$PteGlu$_3$ in the ternary complex is a cation−$\pi$ interaction (*27*). A conserved tryptophan is seen to stack against $CH_3$-$H_4$PteGlu$_3$ in the binary complex (*9*). If this tryptophan is still close to N5 of the folate substrate in the ternary complex, it may also help to raise the $CH_3$-$H_4$PteGlu$_3$ p$K_a$ via a cation−$\pi$ interaction.

*Relevance to Other Enzymes That Use Tertiary Amines as Methyl Donors.* Activation of $CH_3$-$H_4$folate is proposed to proceed via protonation in both cobalamin-dependent and cobalamin-independent methionine synthase as well as in other proteins that utilize $CH_3$-$H_4$folate or other tertiary amines as a methyl donor (*7*, *16*, *28*). These enzymes include the methyltetrahydrofolate:corrinoid Fe/S protein methyltransferase (AcsE), which catalyzes the methylation of the cob(I)amide in the corrinoid Fe/S protein by $CH_3$-$H_4$folate (*29*), and the MtmB, MtbB1, and MttB enzymes involved in generation of methylcorrinoids from monomethylamine, dimethylamine, and trimethylamine, respectively, in *Methanosarcina barkeri* (*30*−*32*). The p$K_a$ values for methylamines suggest that these substrates may bind in the protonated form at neutral pH, although, to our knowledge, this has not been demonstrated for any of these enzymes.

It has been proposed that $CH_3$-$H_4$folate is protonated in the AcsE binary complex, in the absence of the corrinoid Fe/S protein (*28*). NMR spectroscopy indicated that the single, sharp peak of (6*R*,*S*)-[*methyl*-$^{13}$C]$CH_3$-$H_4$folate split into two broader peaks upon titration with AcsE. The chemical shift for the higher field signal was assigned to the *S* isomer and was determined to shift from 42.20 ppm free in solution to 42.58 ppm when bound on AcsE. The authors attributed this 0.38 ppm chemical shift to protonation of $CH_3$-$H_4$folate. However, pH titrations of free (6*R*,*S*)-[*methyl*-$^{13}$C]$CH_3$-$H_4$folate have indicated that protonation of

N5 is accompanied by a much larger chemical shift, 2.1−2.4 ppm, of the $^{13}C$ signal (*16*, *28*).

Seravalli et al. also showed that binding of $CH_3$-$H_4$folate to AcsE was accompanied by proton uptake, suggesting that a proton is involved in the binding. However, the $K_d$ was essentially independent of pH between 4.85 and 8.5, a result that is difficult to reconcile with the proton uptake data. Therefore, the available data neither conclusively refute nor demonstrate that $CH_3$-$H_4$folate is protonated in the AcsE binary complex.

The catalytic strategies of cobalamin-dependent methionine synthase (MetH) and MetE are remarkably similar, despite the lack of sequence similarity in these two enzymes and the marked differences in the mode of folate binding. In both cases, binary enzyme·$CH_3$-$H_4$folate complexes are unprotonated, and protonation occurs only in the presence of the methyl acceptor. Red shifts of the $CH_3$-$H_4$folate spectrum on binding to a fragment of MetH containing only the substrate binding sites indicate that this folate binding site is also relatively hydrophobic and would thus disfavor protonation (*16*). Formation of a complex in which the cob(I)alamin cofactor is positioned to receive the methyl group from $CH_3$-$H_4$folate would introduce a partial negative charge into this hydrophobic environment and thus might favor protonation of $CH_3$-$H_4$folate. Proton transfer is avoided in MetH because the cob(I)alamin nucleophile that is the proximate methyl acceptor has a very low p$K_a$ for protonation of the electrons in the $d_{z^2}$ orbital (*33*, *34*). Although cob(I)alamin is fully activated at neutral pH, the next step in the reaction catalyzed by MetH is nucleophilic attack of Hcy on methylcobalamin. Hcy is activated in MetH, as in MetE, by coordination to a zinc at the active site of the enzyme. Therefore, MetH, the "improbable" enzyme, and MetE, the "impossible" enzyme, appear to employ highly similar strategies to effect catalysis of methyl transfer.

## ACKNOWLEDGMENT

We thank Prof. Bruce A. Palfey for valuable insights and helpful discussions. We also thank Prof. David P. Ballou for help with setup and use of his stopped-flow instrument in the preliminary experiments.

## REFERENCES

1. Benesch, R., and Benesch, R. (1955) The acid strength of the −SH group in cysteine and related compounds, *J. Am. Chem. Soc. 77*, 5877−5881.
2. Roberts, D. D., Lewis, S. D., Ballou, D. P., Olson, S. T., and Shafer, J. A. (1986) Reactivity of small thiolate anions and cysteine-25 in papain toward methyl methanethiosulfonate, *Biochemistry 25*, 5595−5601.
3. Bednar, R. A. (1990) Reactivity and pH dependence of thiol conjugation to *N*-ethylmaleimide: detection of a conformational change in chalcone isomerase, *Biochemistry 29*, 3684−3690.
4. Whitesides, G. M., Lilburn, J. E., and Szajewski, R. P. (1977) Rates of thiol-disulfide interchange reactions between mono- and dithiols and Ellman's reagent, *J. Org. Chem. 42*, 332−338.
5. González, J. C., Peariso, K., Penner-Hahn, J. E., and Matthews, R. G. (1996) Cobalamin-independent methionine synthase from *Escherichia coli*: a zinc metalloenzyme, *Biochemistry 35*, 12228−12234.
6. Goulding, C. W., and Matthews, R. G. (1997) Cobalamin-dependent methionine synthase from *Escherichia coli*: involvement of zinc in homocysteine activation, *Biochemistry 36*, 15749−15757.
7. Matthews, R. G., Smith, A. E., Zhou, Z. S., Taurog, R. E., Bandarian, V., Evans, J. C., and Ludwig, M. (2003) Cobalamin-dependent and cobalamin-independent methionine synthases: are there two solutions to the same chemical problem?, *Helv. Chim. Acta 86*, 3939−3954.
8. Zhou, Z. S., Peariso, K., Penner-Hahn, J. E., and Matthews, R. G. (1999) Identification of the zinc ligands in cobalamin-independent methionine synthase (MetE) from *Escherichia coli*, *Biochemistry 38*, 15915−15926.
9. Pejchal, R., and Ludwig, M. L. (2005) Cobalamin-independent methionine synthase (MetE): a face-to-face double barrel that evolved by gene duplication, *PLoS Biol. 3*, e31.
10. Peariso, K., Zhou, Z. S., Smith, A. E., Matthews, R. G., and Penner-Hahn, J. E. (2001) Characterization of the zinc sites in cobalamin-independent and cobalamin-dependent methionine synthase using zinc and selenium X-ray absorption spectroscopy, *Biochemistry 40*, 987−993.
11. Foster, M. A., Tejerina, G., Guest, J. R., and Woods, D. D. (1964) Two enzymic mechanisms for the methylation of homocysteine by extracts of *Escherichia coli*, *Biochem. J. 92*, 476−488.
12. Whitfield, C. D., Steers, E. J., Jr., and Weissbach, H. (1970) Purification and properties of 5-methyltetrahydropteroyltriglutamate-homocysteine transmethylase, *J. Biol. Chem. 245*, 390−401.
13. Furness, R. A., and Loewen, P. C. (1981) Detection of *p*-aminobenzoylpoly(gamma-glutamates) using fluorescamine, *Anal. Biochem. 117*, 126−135.
14. Ferrer, J. L., Ravanel, S., Robert, M., and Dumas, R. (2004) Crystal structures of cobalamin-independent methionine synthase complexed with zinc, homocysteine, and methyltetrahydrofolate, *J. Biol. Chem. 279*, 44235−44238.
15. Kallen, R. G., and Jencks, W. P. (1966) The dissociation constants of tetrahydrofolic acid, *J. Biol. Chem. 241*, 5845−5850.
16. Smith, A. E., and Matthews, R. G. (2000) Protonation state of methyltetrahydrofolate in a binary complex with cobalamin-dependent methionine synthase, *Biochemistry 39*, 13880−13890.
17. Evans, J. C., Huddler, D. P., Hilgers, M. T., Romanchuk, G., Matthews, R. G., and Ludwig, M. L. (2004) Structures of the N-terminal modules imply large domain motions during catalysis by methionine synthase, *Proc. Natl. Acad. Sci. U.S.A. 101*, 3729−3736.
18. Patil, P. V., and Ballou, D. P. (2000) The use of protocatechuate dioxygenase for maintaining anaerobic conditions in biochemical experiments, *Anal. Biochem. 286*, 187−192.
19. Palfey, B. A. (2003) Time-resolved spectral analysis, in *Kinetic Analysis of Macromolecules* (Johnson, K. A., Ed.) Oxford University Press, Oxford.
20. Segal, I. H. (1993) *Enzyme Kinetics: Behavior and Analysis of Rapid Equilibrium and Steady-State Enzyme Systems*, Wiley-Interscience, New York.
21. Miller, R. J., Kuliopulos, A., and Coward, J. K. (1989) Alkyltransferase model reactions: synthesis of sulfonium and ammonium compounds containing neighboring nucleophiles. Kinetic studies of the intramolecular reaction of amino, hydroxy, phenoxy, and mercapto onium salts, *J. Org. Chem. 54*, 3436−3448.
22. Callahan, B. P., and Wolfenden, R. (2003) Migration of methyl groups between aliphatic amines in water, *J. Am. Chem. Soc. 125*, 310−311.
23. Budavari, S., O'Neil, M. J., Smith, A., and Heckelman, P. E., Eds. (1989) *The Merck Index: An Encyclopedia of Chemicals, Drugs, and Biologicals*, Merck & Co., Rahway, NJ.
24. Orttung, W. H. (1969) Interpretation of the titration curve of oxyhemoglobin. Detailed consideration of Coulomb interactions at low ionic strength, *J. Am. Chem. Soc. 91*, 162−167.
25. Li, J., Nelson, M. R., Peng, C. Y., Bashford, D., and Noodleman, L. (1998) Incorporating protein environments in density functional theory: A self-consistent reaction field calculation of redox potentials of [2Fe2S] clusters in ferredoxin and phthalate dioxygenase reductase, *J. Phys. Chem. A 102*, 6311−6324.
26. Honig, B. H., Hubbell, W. L., and Flewelling, R. F. (1986) Electrostatic interactions in membranes and proteins, *Annu. Rev. Biophys. Biophys. Chem. 15*, 163−193.
27. Kumpf, R. A., and Dougherty, D. A. (1993) A mechanism for ion selectivity in potassium channels: computational studies of cation-pi interactions, *Science 261*, 1708−1710.
28. Seravalli, J., Shoemaker, R. K., Sudbeck, M. J., and Ragsdale, S. W. (1999) Binding of (6*R*,*S*)-methyltetrahydrofolate to methyltransferase from *Clostridium thermoaceticum*: role of protonation of methyltetrahydrofolate in the mechanism of methyl transfer, *Biochemistry 38*, 5736−5745.

29. Hu, S. I., Pezacka, E., and Wood, H. G. (1984) Acetate synthesis from carbon monoxide by *Clostridium thermoaceticum*. Purification of the corrinoid protein, *J. Biol. Chem. 259*, 8892−8897.
30. Burke, S. A., and Krzycki, J. A. (1997) Reconstitution of monomethylamine:coenzyme M methyl transfer with a corrinoid protein and two methyltransferases purified from *Methanosarcina barkeri*, *J. Biol. Chem. 272*, 16570−16577.
31. Ferguson, D. J., Jr., Gorlatova, N., Grahame, D. A., and Krzycki, J. A. (2000) Reconstitution of dimethylamine:coenzyme M methyl transfer with a discrete corrinoid protein and two methyltransferases purified from *Methanosarcina barkeri*, *J. Biol. Chem. 275*, 29053−29060.
32. Ferguson, D. J., Jr., and Krzycki, J. A. (1997) Reconstitution of trimethylamine-dependent coenzyme M methylation with the trimethylamine corrinoid protein and the isozymes of methyltransferase II from *Methanosarcina barkeri*, *J. Bacteriol. 179*, 846−852.
33. Tackett, S. L., Collat, J. W., and Abbott, J. C. (1963) The formation of hydridocobalamin and its stability in aqueous solutions, *Biochemistry 2*, 919−923.
34. Lexa, D., and Saveant, M. (1983) The electrochemistray of vitamin B12, *Acc. Chem. Res. 16*, 235−243.
35. Taurog, R. E., Jakubowski, H., and Matthews, R. G. (2006) Synergistic, random sequential binding of substrates in cobalamin-independent methionine synthase, *Biochemistry 45*, 5083−5091.

BI060052M